From direct to indirect searches for new physics in beauty decays

Anne-Mazarine Lyon

CERN

MBI Seminar

29^{th} May 2026

Context

- The standard model of particle physics is not a complete theory!
  - Does not incorporate a description of gravity
  - Does not provide explanations for fundamental questions

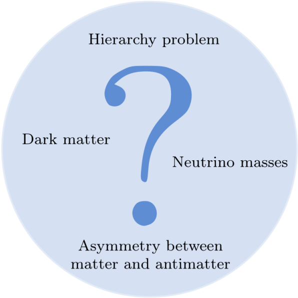

... and many more!

- Possible extensions of the standard model are referred to as **new physics**

My expertise

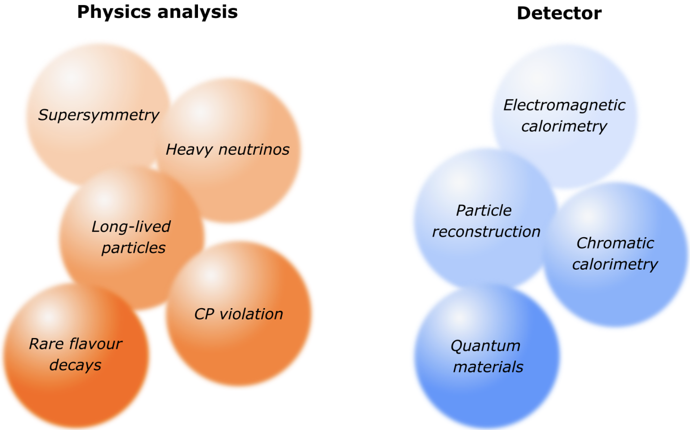

- In this talk, I will focus on
  - Direct and indirect searches for new physics in beauty decays at CMS
  - Chromatic calorimetry using nanocomposites, a novel particle sensing technology for future detectors at the FCC-ee

CMS experiment

- General-purpose experiment at the CERN LHC
  - Proton-proton collisions
  - Run 2 (2016–2018, $\sqrt{s} = 13$ TeV), Run 3 (2022–2026, $\sqrt{s} = 13.6$ TeV)
- Particle content reconstructed using information from different subdetectors

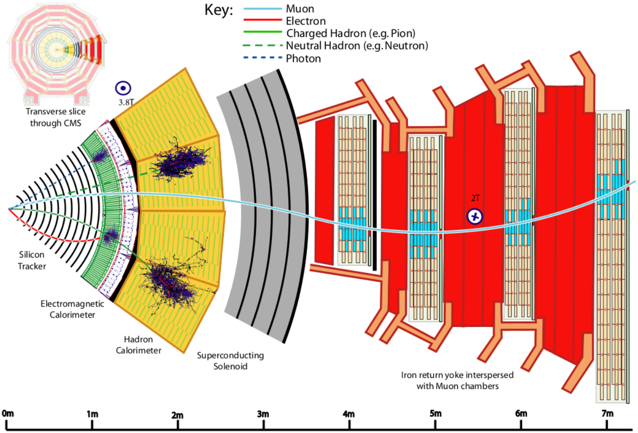

doi:10.1088/1748-0221/12/10/P10003

Beauty physics at CMS

- Decays of particles containing a beauty (b) quark are a key portal to probe new physics
- CMS has established a diversified flavour physics programme
  - Virtually 4π solid-angle coverage and large recorded luminosity
  - Excellent vertexing performance
  - Outstanding muon reconstruction and identification

Beauty physics at CMS

- Decays of particles containing a beauty (b) quark are a key portal to probe new physics
- CMS has established a diversified flavour physics programme
  - Virtually 4π solid-angle coverage and large recorded luminosity
  - Excellent vertexing performance
  - Outstanding muon reconstruction and identification
- Large efforts in deploying triggers with low thresholds on the transverse momentum (p_{T}) (B-parking data sets, (arXiv:2403.16134))
  - Large data set of $\mathrm{B\overline{B}}$ pairs
  - In particular, trigger on single-muon

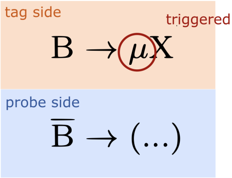

$\Rightarrow$ **Unprecedented possibility to study B decays at CMS**

Outline

- This talk is organised in three parts

I. Direct search for new physics

Search for long-lived heavy neutrinos in beauty decays

II. Indirect search for new physics

CP violation measurement in all-hadronic $\mathrm{B_s} \to \phi\phi$ *decays*

III. Quantum sensing

Towards chromatic calorimetry using nanocomposites

I. Direct search for new physics

Search for long-lived heavy neutrinos in beauty decays

Motivation for heavy neutrinos

- Flavour oscillation of neutrinos

$\alpha, \beta = (e, \mu, \tau)$

  - At least two neutrinos are massive

Motivation for heavy neutrinos

- Flavour oscillation of neutrinos

$\alpha, \beta = (e, \mu, \tau)$

  - At least two neutrinos are massive

- How to generate the mass of the neutrinos?
  - A possible mechanism is the *Type I seesaw mechanism*
  - Introduction of **heavy neutrinos / heavy neutral leptons (HNLs)**

$$\mathcal{L}_{\text{mass}} = -\frac{1}{2} \begin{pmatrix} \overline{\nu}_{\text{L}} & \overline{\nu}^{\text{c}}_{\text{R}} \end{pmatrix} \begin{pmatrix} 0 & m_{\text{D}} \\ m_{\text{D}}^{\text{T}} & M_{\text{M}} \end{pmatrix} \begin{pmatrix} \nu^{\text{c}}_{\text{L}} \\ \nu_{\text{R}} \end{pmatrix} + \text{h.c.}$$

$M_{\text{M}} \gg m_{\text{D}}$

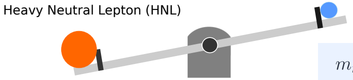

$$m_\nu = \frac{m_{\text{D}}^2}{M_{\text{M}}}$$
$$\nu \approx (\nu_L + \nu_L^c)$$

$$m_{\text{HNL}} = M_{\text{M}}$$
$$\text{HNL} \approx (\nu_{\text{R}} + \nu^{\text{c}}_{\text{R}})$$

Motivation for heavy neutrinos

- Flavour oscillation of neutrinos

$\alpha, \beta = (e, \mu, \tau)$

  - At least two neutrinos are massive

- How to generate the mass of the neutrinos?
  - A possible mechanism is the *Type I seesaw mechanism*
  - Introduction of **heavy neutrinos / heavy neutral leptons (HNLs)**

Neutrino minimal standard model

- Masses of heavy neutrinos in the GeV scale
- HNLs interact through mixing with SM neutrinos

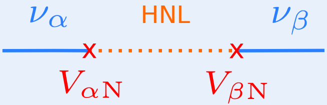

Experimental landscape

- Phenomenology described with four parameters: m_{N}, V_{eN}, $V_{\mu\mathrm{N}}$, $V_{\tau\mathrm{N}}$
- $|V_{\mathrm{N}}|^2 = |V_{\mathrm{eN}}|^2 + |V_{\mu\mathrm{N}}|^2 + |V_{\tau\mathrm{N}}|^2$; Lifetime $\tau_{\mathrm{N}} \sim m_{\mathrm{N}}^{-5}|V_{\mathrm{N}}|^{-2}$

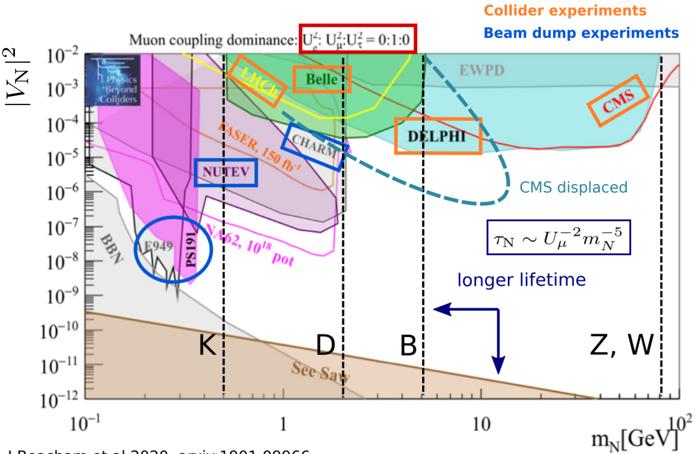

J Beacham et al 2020, arxiv:1901.09966

Experimental landscape

- Phenomenology described with four parameters: $m_{\rm N}$, $V_{\rm eN}$, $V_{\mu\rm N}$, $V_{\tau\rm N}$
- $|V_{\rm N}|^2 = |V_{\rm eN}|^2 + |V_{\mu\rm N}|^2 + |V_{\tau\rm N}|^2$; Lifetime $\tau_{\rm N} \sim m_{\rm N}^{-5}|V_{\rm N}|^{-2}$

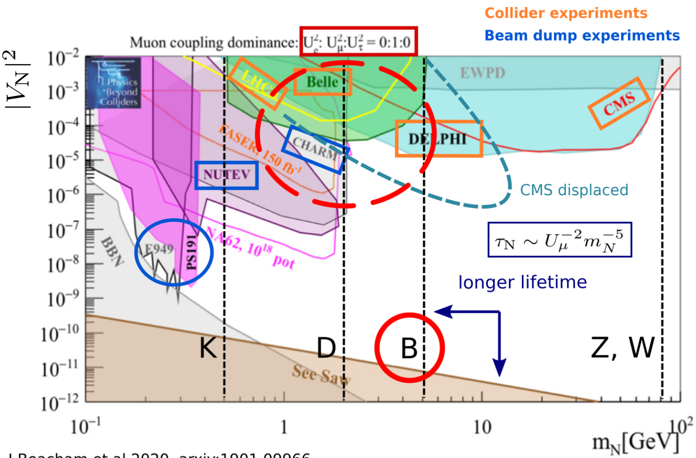

J Beacham et al 2020, arxiv:1901.09966

Experimental landscape

- Phenomenology described with four parameters: m_{N}, V_{eN}, $V_{\mu\mathrm{N}}$, $V_{\tau\mathrm{N}}$
- $|V_{\mathrm{N}}|^2 = |V_{\mathrm{eN}}|^2 + |V_{\mu\mathrm{N}}|^2 + |V_{\tau\mathrm{N}}|^2$; Lifetime $\tau_{\mathrm{N}} \sim m_{\mathrm{N}}^{-5}|V_{\mathrm{N}}|^{-2}$

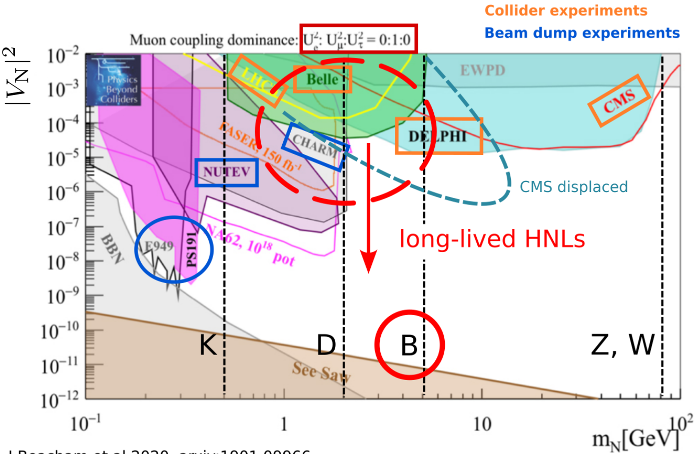

J Beacham et al 2020, arxiv:1901.09966

Scope and challenges

First search for heavy neutrinos in the decays of B mesons performed at a general-purpose experiment at the LHC

Why it is a promising discovery channel:

- Abundant source of SM neutrinos
- Products of such decays have a better acceptance

Challenges:

- Handle the signatures of B physics processes
- Long-lived particle decay gives rise to complex signatures
- A large sample of $b\bar{b}$ events is crucial $\Rightarrow$ use the tag side of the 2018 B-parking data set

Process

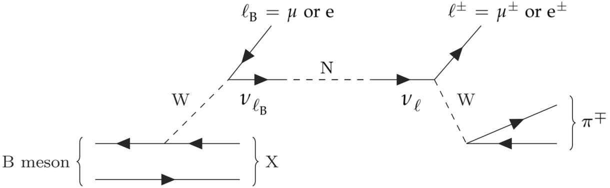

Process

- Inclusive B meson decay

$B \to \mu\nu_R$
$B \to D^0\mu\nu_R$
$B^0 \to \pi\nu_R$
$B_s \to K\mu\nu_R$
...

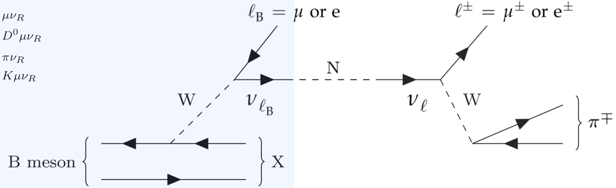

- Inclusive leptonic and semileptonic decays of $B^\pm$, B^0, B_s, and B_c mesons

Process

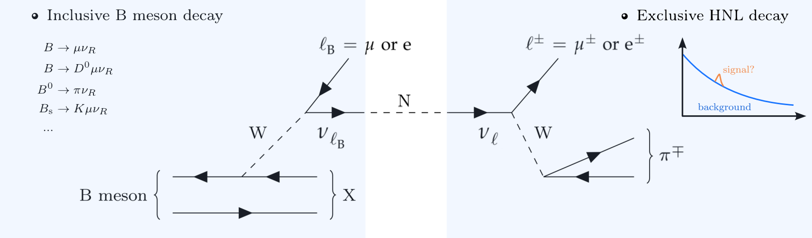

- Inclusive leptonic and semileptonic decays of $B^\pm$, B^0, B_s, and B_c mesons
- Perform a **bump hunt** in the $\ell\pi$ invariant mass spectrum
  - Masses probed in the range $1 < m_N < 6$ GeV with unprecedented resolution

Process

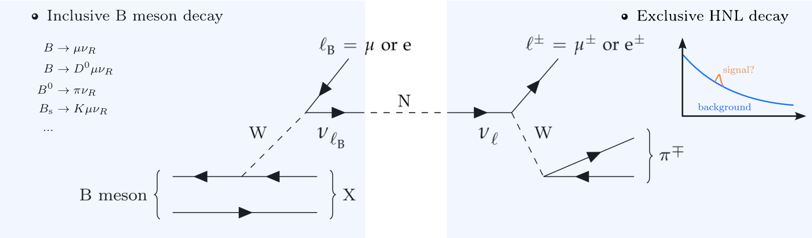

- Inclusive leptonic and semileptonic decays of $B^\pm$, B^0, B_s, and B_c mesons
- Perform a **bump hunt** in the $\ell\pi$ invariant mass spectrum
  - Masses probed in the range $1 < m_N < 6$ GeV with unprecedented resolution
- At least one lepton is a μ that fires a B-parking trigger line
  - $B \to \mu_B NX$, $N \to \mu^\pm \pi^\mp$ $\Rightarrow$ dimuon channel
  - $B \to \mu_B NX$, $N \to e^\pm \pi^\mp$ } mixed-flavour channel
  - $B \to e_B NX$, $N \to \mu^\pm \pi^\mp$ }

Process

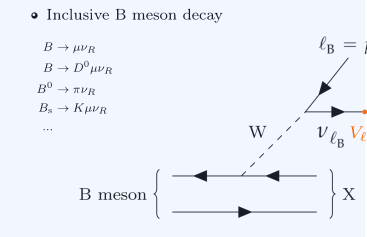

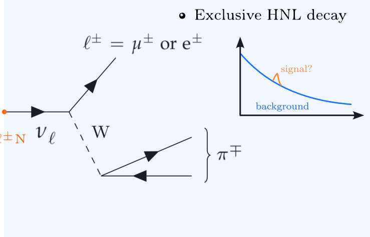

- Inclusive leptonic and semileptonic decays of $B^\pm$, B^0, B_s, and B_c mesons
- Perform a **bump hunt** in the $\ell\pi$ invariant mass spectrum
  - Masses probed in the range $1 < m_N < 6$ GeV with unprecedented resolution
- At least one lepton is a μ that fires a B-parking trigger line
  - $B \to \mu_B NX$, $N \to \mu^\pm\pi^\mp \Rightarrow$ dimuon channel
  - $B \to \mu_B NX$, $N \to e^\pm\pi^\mp$ } mixed-flavour channel
  - $B \to e_B NX$, $N \to \mu^\pm\pi^\mp$ } mixed-flavour channel
- Interpret the results against **mixed-flavour** mixing scenarios

Process

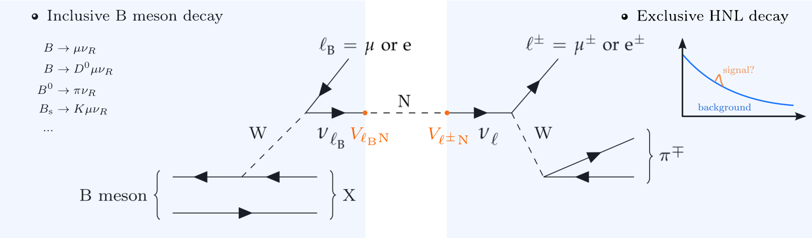

- Inclusive leptonic and semileptonic decays of $B^\pm$, B^0, B_s, and B_c mesons
- Perform a **bump hunt** in the $\ell\pi$ invariant mass spectrum
  - Masses probed in the range $1 < m_N < 6$ GeV with unprecedented resolution
- At least one lepton is a μ that fires a B-parking trigger line
  - $B \to \mu_B NX$, $N \to \mu^\pm\pi^\mp$ $\Rightarrow$ dimuon channel
  - $B \to \mu_B NX$, $N \to e^\pm\pi^\mp$
  - $B \to e_B NX$, $N \to \mu^\pm\pi^\mp$

  } mixed-flavour channel
- Interpret the results against **mixed-flavour** mixing scenarios
- HNL may either be a Majorana or a Dirac-like particle

Strategy

1. Reconstruct the signal candidates

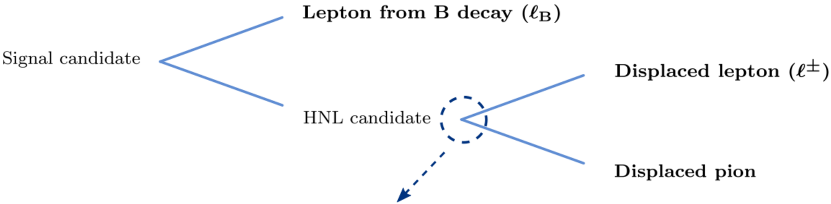

- Displaced pion and lepton fitted to a common vertex using a *kinematic vertex fitter*

- The efficiency of the signal candidate reconstruction reaches a few percent for transverse displacement $L_{xy} > 50$ cm

Strategy

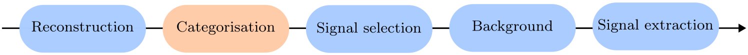

2. Categorise the events to enhance sensitivity on different signal hypotheses

Quantity	Label	Definition
$L_{xy}/\sigma_{L_{xy}}$	low $L_{xy}/\sigma_{L_{xy}}$ medium $L_{xy}/\sigma_{L_{xy}}$ high $L_{xy}/\sigma_{L_{xy}}$	$L_{xy}/\sigma_{L_{xy}} < 50$ $50 < L_{xy}/\sigma_{L_{xy}} < 150$ $L_{xy}/\sigma_{L_{xy}} > 150$
Relative lepton sign	OS SS	ℓ_B charge $\neq \ell$ charge ℓ_B charge $= \ell$ charge
$\ell_B\ell^\pm\pi^\mp$ mass	low $\ell_B\ell^\pm\pi^\mp$ mass high $\ell_B\ell^\pm\pi^\mp$ mass	$\ell_B\ell^\pm\pi^\mp$ mass < 5.7 GeV $\ell_B\ell^\pm\pi^\mp$ mass > 5.7 GeV
Flavour channel	dimuon mixed-flavour	$\ell_B\ell = \mu\mu$ $\ell_B\ell = (\mu e, e\mu)$

- Emphasizes signals with different lifetime hypotheses

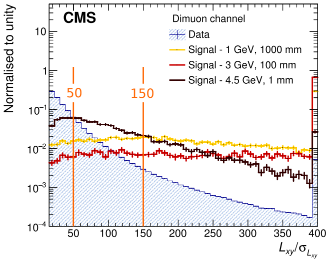

Strategy

Reconstruction — Categorisation — **Signal selection** — Background — Signal extraction

3. Reject the background while preserving the large variety of signal signatures

- The different signal hypotheses (m_{N}, $c\tau_{\mathrm{N}}$) can give rise to significantly different signatures

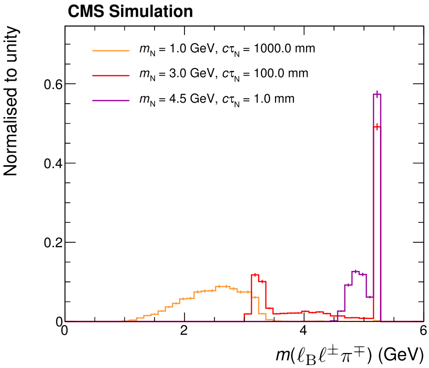

Strategy

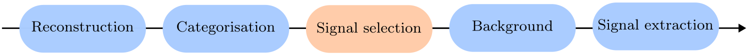

3. Reject the background while preserving the large variety of signal signatures
   - Implementation of an algorithm based on machine learning
   - Takes as input highly discriminating kinematic and topological variables

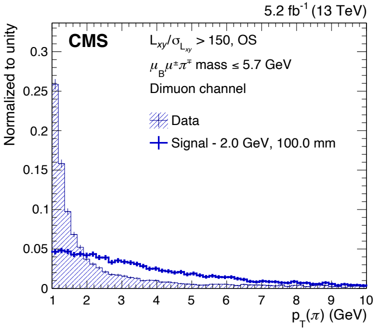

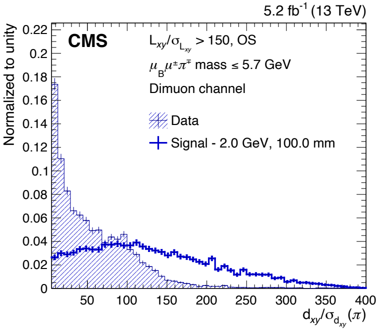

Strategy

Reconstruction — Categorisation — **Signal selection** — Background — Signal extraction →

3. Reject the background while preserving the large variety of signal signatures

- Selection algorithm based on parametric Neural Networks (pNNs) (arXiv:1601.07913)
  - NNs with extra discrete parameter that is concatenated to the features
  - Allows a single training for different signal hypotheses
  - Maintains good performance for the intermediate signal points
- Separate pNN trainings in the different analysis categories
- Events are selected if pNN score > 0.99

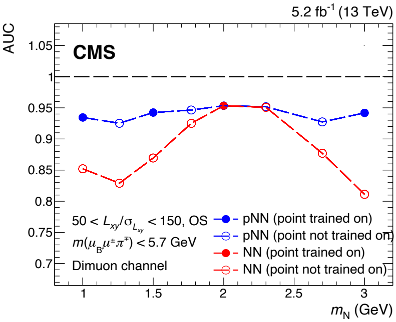

Strategy

Reconstruction → Categorisation → Signal selection → Background → Signal extraction

3. Reject the background while preserving the large variety of signal signatures

- Selection algorithm based on parametric Neural Networks (pNNs) (arXiv:1601.07913)
  - NNs with extra discrete parameter that is concatenated to the features
  - Allows a single training for different signal hypotheses
  - Maintains good performance for the intermediate signal points
- Separate pNN trainings in the different analysis categories
- Events are selected if pNN score > 0.99

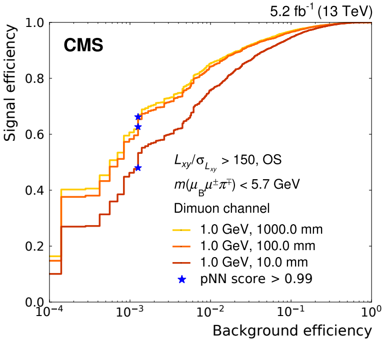

Strategy

Reconstruction → Categorisation → Signal selection → **Background** → Signal extraction

4. Model the background

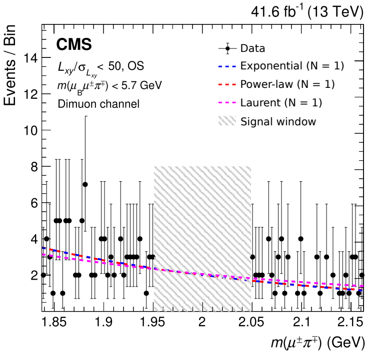

- Background primarily arises from
  - B cascade decays
  - Combinatorial processes
- Parametric fit to the data

Strategy

Reconstruction → Categorisation → Signal selection → Background → **Signal extraction**

5. Extract the signal

- Extract signal for ~ 100 mass hypotheses in $1 < m_\mathrm{N} < 6$ GeV in step of twice the mass resolution, σ
- When probing an HNL of mass M, extract signal in a mass window of size $\pm 10\sigma$ centred at M
- Select events using pNN evaluated at mass M
- Model the background from the mass sidebands
- Extract signal with simultaneous maximum likelihood fits to $m(\ell^{\pm}\pi^{\mp})$ in each event category

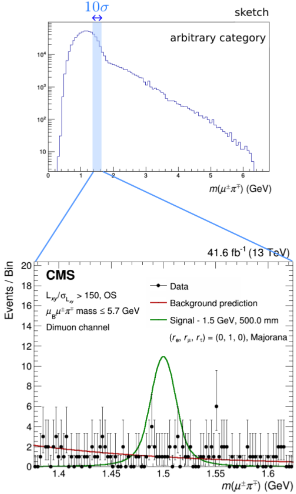

Results

- No significant excess from the predicted background is observed in any of the $\ell^{\pm}\pi^{\mp}$ invariant mass distributions

1

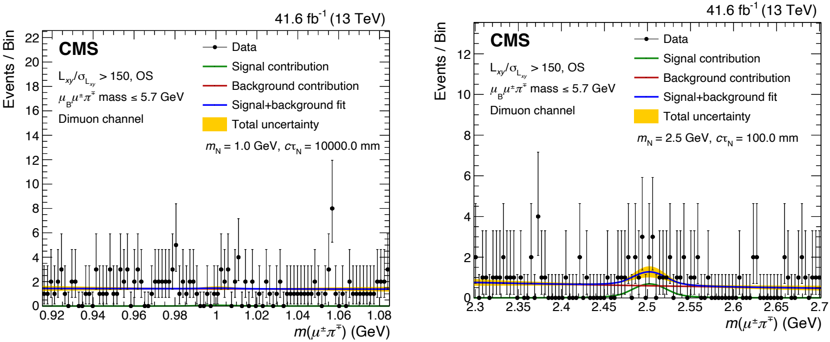

10.1007/JHEP06(2024)183, 10.1016/j.physrep.2024.09.012, 10.1016/j.physrep.2024.09.006

Interpretation

- Upper exclusion limits at 95% CL on $|V_N|^2$ are presented for the muon-exclusive mixing scenario, and for both the Majorana and Dirac hypotheses

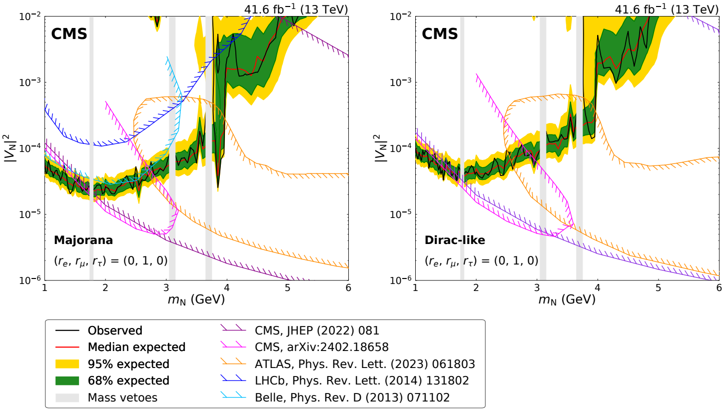

$\Rightarrow$ **Most stringent limits obtained in the mass range $1 < m_N < 1.7$ GeV at a collider experiment to date**

II. Indirect search for new physics

CP violation measurement in all-hadronic $\mathrm{B_s} \to \phi\phi$ *decays*

Indirect searches

- New physics can also be searched for in an indirect way
- Precision is key !
  - Precise SM predictions are needed...
  - ... as well as precise experimental measurements
- A deviation of the measurement to the theoretical prediction interpreted as a sign for new physics in the data
- Two of the main advantages of this approach
  1. It can probe new particles with masses beyond the actual reach of the accelerator
  2. It is model independent

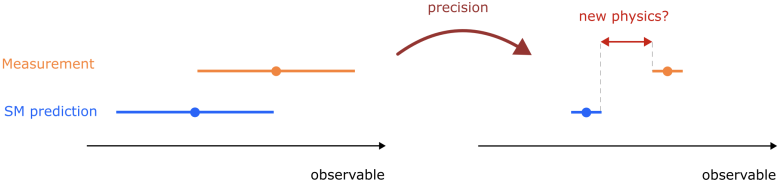

CP violation (CPV)

- The violation of charge-parity (CP) symmetry is
  - One of Sakharov's conditions to explain the matter/antimatter imbalance in the Universe
  - A good observable to probe new physics via precision measurements
- CPV measurements **at CMS** in charm and beauty sectors
  - CMS achieves competitive precision with respect to flavour-dedicated experiments!

Sector	Channel	Ref.
CHARM	$D^0 \to \mathrm{K_S K_S}$	paper
BEAUTY	$\mathrm{B_s} \to \mathrm{J}/\psi\phi$	paper
	$\mathrm{B} \to \mathrm{J}/\psi \mathrm{K_S}$	Talk at LHCP 2026

- In the **beauty sector**, CPV measurements were so far based on dimuon resonances

Can penguin-dominated decays be used at CMS for CPV measurements in the beauty sector?

Motivation for the $B_s \to \phi\phi$ channel

- Penguin-dominated process
  - Enhanced sensitivity to new physics (10.1103/PhysRevD.88.016007)

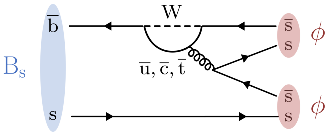

Unmixed $B_s \to \phi\phi$ *decay*

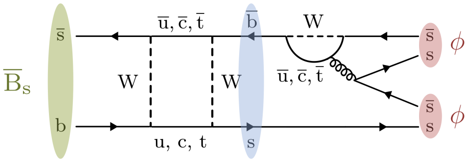

Mixed $\overline{B}_s \to B_s \to \phi\phi$ *decay*

- Benchmark channel to study time-dependent CP violation in flavour-changing neutral current in $b \to s\bar{s}s$ transitions

- CPV arises from the interference between the direct decay and the decay after B_s mixing

$$\Gamma\left(B_s(\rightsquigarrow \overline{B}_s) \to \phi\phi\right)(t) \overset{?}{\neq} \Gamma\left(\overline{B}_s(\rightsquigarrow B_s) \to \phi\phi\right)(t)$$

- Allows for measurement of angle $\phi_s \equiv \phi_s^{s\bar{s}s}$ and direct CPV parameter $|\lambda|$

State of the art

- LHCb has published a CPV measurement in $B_s \to \phi\phi$ decays using the Run 1+Run 2 data sets (paper)
  - Using the $B_s \to \phi(K^+K^-)\phi(K^+K^-)$ channel
- Measurement is statistically limited

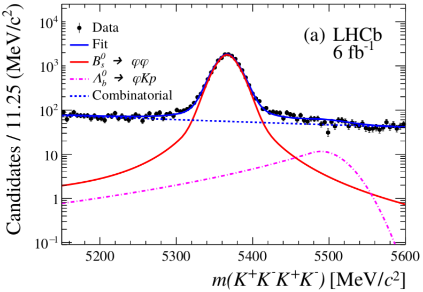

Parameter	Result
$\phi_s^{s\bar{s}s}$ [rad]	$-0.042 \pm 0.075 \pm 0.009$
$\lvert\lambda\rvert$	$1.004 \pm 0.030 \pm 0.009$
$\lvert A_0\rvert^2$	$0.384 \pm 0.007 \pm 0.003$
$\lvert A_\perp\rvert^2$	$0.310 \pm 0.006 \pm 0.003$
$\delta_\parallel - \delta_0$ [rad]	$2.463 \pm 0.029 \pm 0.009$
$\delta_\perp - \delta_0$ [rad]	$2.769 \pm 0.105 \pm 0.011$

LHCb Run 1 + Run 2 results

$\Rightarrow$ Can CMS measure with a similar precision?

Decay channel

- $\phi \to K^+K^-$ decay channel is considered
  - Much larger cross section than $\phi \to \mu\mu$ channel as $\mathcal{B}(\phi \to KK) \sim 5 \times 10^{-1}$
  - Overwhelming combinatorial background is expected
  - Exploit the probe side of Run 2 + Run 3 single-muon B-parking data set ($\sim$ 220 fb^{-1})

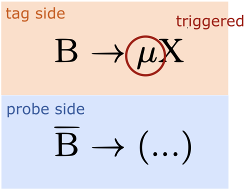

Signal simulation

- The $B_s \to \phi(K^+K^-)\phi(K^+K^-)$ signal is simulated using Pythia + EvtGen generators
- Because ϕ mesons are *vector* particles, polarisation effects must be included
  - Use the `EvtPVVCPLH` decay model of EvtGen

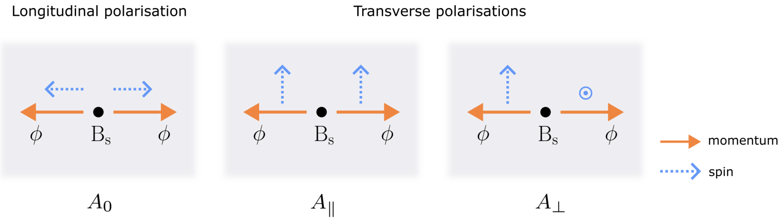

Reconstruction

- Signal candidates reconstructed in a two-step manner
  1. First, reconstruct $\phi \to$ KK candidates
  2. Then, reconstruct $\mathrm{B_s} \to \phi\phi$ candidates

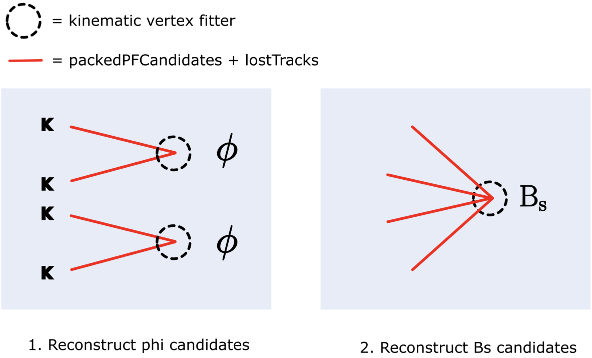

- Reconstruction efficiency of about 70%

Preselection

- A series of cuts are applied to preselect interesting events

phi candidates

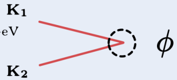

- $p_T > 0.8$ GeV (K_1)
- $p_T > 0.7$ GeV (K_2)
- $|m(K_1K_2) - 1.02| < 120$ MeV
- $\Delta R(K_1K_2) < 0.25$
- prob > 0.01

Bs candidates

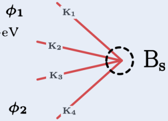

- $p_T > 2.5$ GeV (ϕ_1)
- $p_T > 1.8$ GeV (ϕ_2)
- $p_T(\phi_1) \times p_T(\phi_2) > 6$ GeV
- $p_T > 1.5$ GeV
- $|\eta| < 2.5$
- $\min(\Delta R(K_1K_2K_3PK_4)) < 0.15$
- $\max(\Delta R(K_1K_2K_3PK_4)) < 2.5$
- $L_{xy}/\sigma_{L_{xy}} > 1$
- prob > 0.001

- Preselection cuts not efficient enough to isolate the signal over the overwhelming background
  - Employ a multivariate algorithm

Selection

- Selection algorithm based on a deep neural network (NN)
- Use discriminating variables as training features

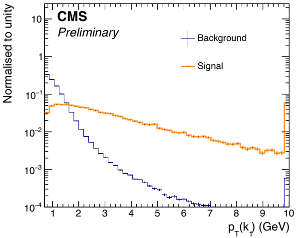

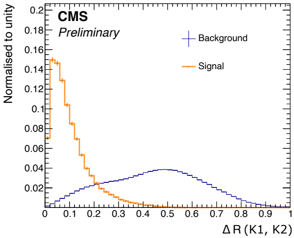

- NN achieves good signal-to-background separation
- Events selected with NN score > 0.96

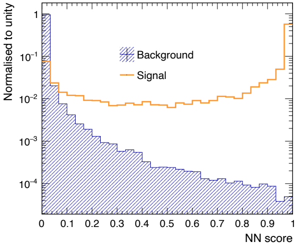

Context
CMS
Part I
Part II
Context
CPV
Motivation
Landscape
Channel
Simulation
Reconstruction
Preselection
Selection
Mass
Tagging
Sensitivity
Outlook
Part III
Summary
Backup

Flavour tagging

- The CP asymmetry can be expressed as

$$a_{\mathrm{CP}}(t) = \frac{\Gamma\left(\mathrm{B_s} \to \phi\phi\right)(t) - \Gamma\left(\overline{\mathrm{B}}_\mathrm{s} \to \phi\phi\right)(t)}{\Gamma\left(\mathrm{B_s} \to \phi\phi\right)(t) + \Gamma\left(\overline{\mathrm{B}}_\mathrm{s} \to \phi\phi\right)(t)}$$

- In an event, one must identify whether the $\phi\phi$ resonance originates from a $\mathrm{B_s}$ or $\overline{\mathrm{B}}_\mathrm{s}$ decay
  - This procedure falls under the name of *flavour tagging*
- The strategy consists in inferring the flavour of the $\mathrm{B_s}$ meson from
  - The knowledge of the charge of the tag muon
  - The conservation of the beauty quantum number
- Preliminary studies show that the tagging efficiency lies around $\sim 20\%$

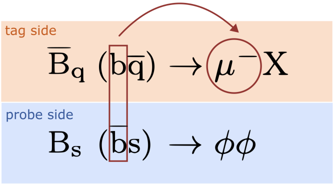

Outlook

- The feasibility study shows that CMS is capable of doing flavour physics using fully hadronic final states
- Another interesting decay is $\mathrm{B_d} \to \phi(\mathrm{KK})\mathrm{K_S}(\pi\pi)$
  - Also penguin-dominated
  - Allows for measurement of $\sin(2\beta)$
- It also motivates the introduction of all-hadronic triggers during HL-LHC
  - Made possible through CMS detector upgrade
  - Tracking and vertexing information will then be available at the first level trigger

III. Quantum sensing

Towards chromatic calorimetry using nanocomposites

European Pathfinder Open project UNICORN (GA 101098649)

Basics of electromagnetic calorimetry

- An electromagnetic calorimeter is a detector that
  - Aims to measure the energy of an incoming particle...
  - ...by fully absorbing it through the initiation of shower of secondary particles

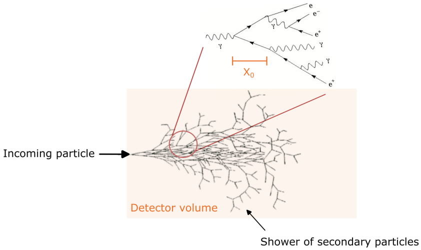

- Two types of electromagnetic calorimeters

Homogeneous calorimeters

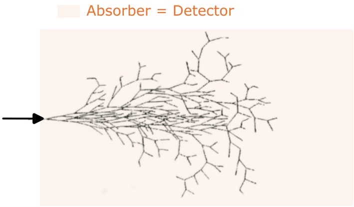

Sampling calorimeters

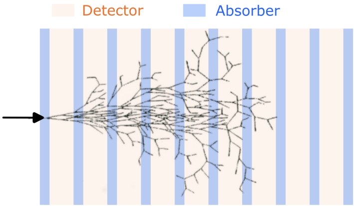

Basics of electromagnetic calorimetry

- An electromagnetic calorimeter is a detector that
  - Aims to measure the energy of an incoming particle...
  - ...by fully absorbing it through the initiation of shower of secondary particles

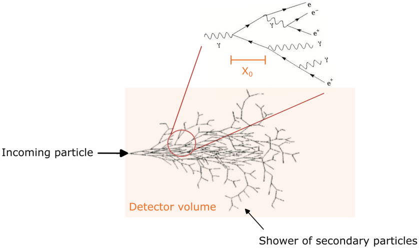

- Two types of electromagnetic calorimeters

Homogeneous calorimeters

- Good energy resolution
- No spatial resolution in the longitudinal direction of the shower development

Sampling calorimeters

- Limited energy resolution
- Longitudinal resolution of the shower possible

Basics of electromagnetic calorimetry

- An electromagnetic calorimeter is a detector that
  - Aims to measure the energy of an incoming particle...
  - ...by fully absorbing it through the initiation of shower of secondary particles

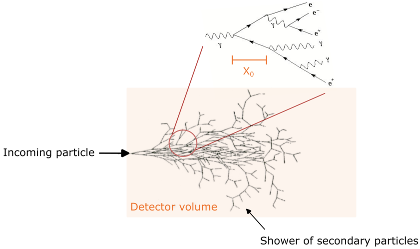

- Two types of electromagnetic calorimeters

Homogeneous calorimeters

- Good energy resolution
- No spatial resolution in the longitudinal direction of the shower development

Sampling calorimeters

- Limited energy resolution
- Longitudinal resolution of the shower possible

Objective

⇒ Can we build a homogeneous calorimeter with longitudinal segmentation?

Concept of chromatic calorimetry

- A chromatic calorimeter (CCAL) is made of successive layers of scintillating materials that emit light within a specific wavelength (λ) range (paper)
- Readout capable of discriminating signals with different λ
- The amount of light collected per colour allows for the reconstruction of the shower profile

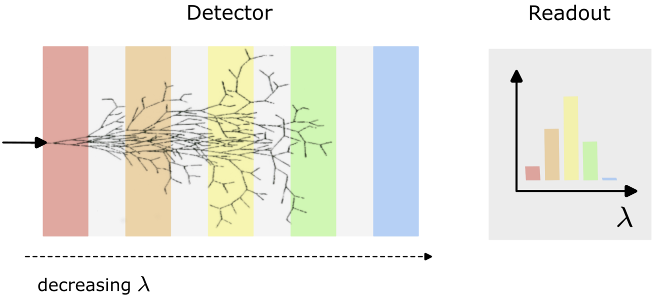

$\Rightarrow$ Shower profile can be resolved in the longitudinal direction, while preserving a good energy resolution

Proof of concept

- To test the concept of chromatic calorimetry, a CCAL prototype was tested using standard materials
  - Plastic and crystal scintillators with well-understood optical properties
- The CCAL prototype was tested in September 2025 at the CERN SPS
- Several high-energy beams were used
  - Electrons at 10, 20, 40, 60, 80, 100, and 120 GeV
  - Charged pions at 80 GeV

Proof of concept – Prototype

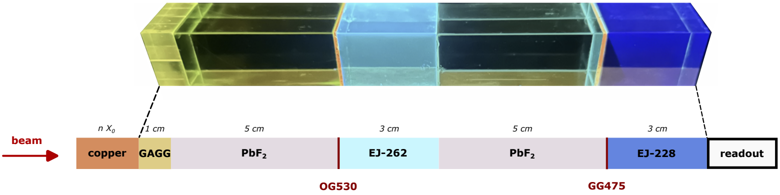

Proof of concept – Prototype

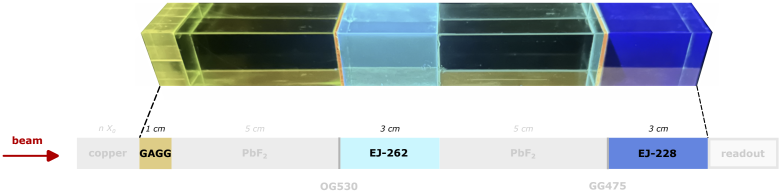

- 3-layered prototype built with standard materials emitting in different λ-ranges
  - Crystal scintillator: GAGG
  - Plastic scintillators: EJ-262 and EJ-228

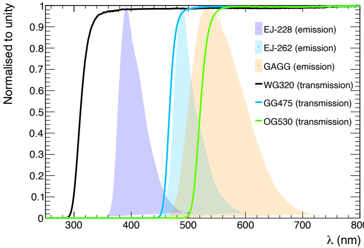

Proof of concept – Prototype

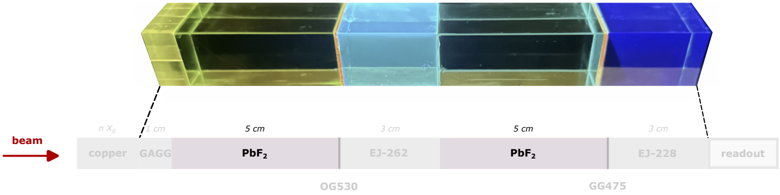

- 3-layered prototype built with standard materials emitting in different λ-ranges
  - Crystal scintillator: GAGG
  - Plastic scintillators: EJ-262 and EJ-228
- PbF_2 used as a dense transparent absorber

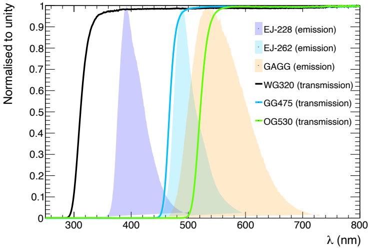

Proof of concept – Prototype

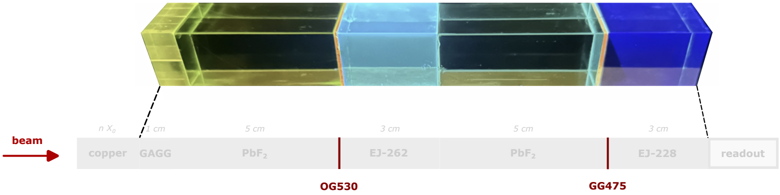

Context
CMS
Part I
Part II
Part III
Calorimetry
Chromatic calorimetry
Proof of concept
Nanocomposites
Materials
Properties
WLS
Outlook
Summary
Backup

- 3-layered prototype built with standard materials emitting in different λ-ranges
  - Crystal scintillator: GAGG
  - Plastic scintillators: EJ-262 and EJ-228
- PbF_2 used as a dense transparent absorber
- Long-pass filters placed to minimise the impact of *echo photons*
  - Photons emitted backward from a scintillator that might that might excite the preceding scintillator

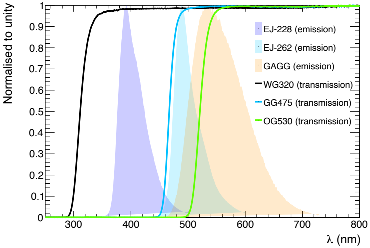

Proof of concept – Prototype

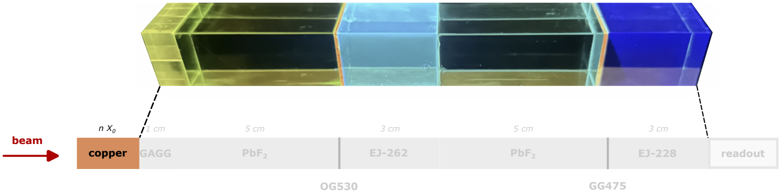

- 3-layered prototype built with standard materials emitting in different λ-ranges
  - Crystal scintillator: GAGG
  - Plastic scintillators: EJ-262 and EJ-228
- PbF_2 used as a dense transparent absorber
- Long-pass filters placed to minimise the impact of *echo photons*
  - Photons emitted backward from a scintillator that might that might excite the preceding scintillator
- Copper absorber of length $n \times X_0$, $n \in [1, 3, 9.9]$, used as a preshower

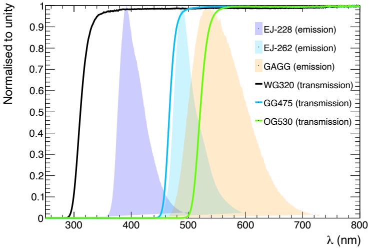

Proof of concept – Readout

- Signal collected with a 4-anode photomultiplier (PMT)
- Long-pass filters placed in front of 3 of the anodes to select light within a given λ-range
  - Their transmittance does not exhibit an angular dependency

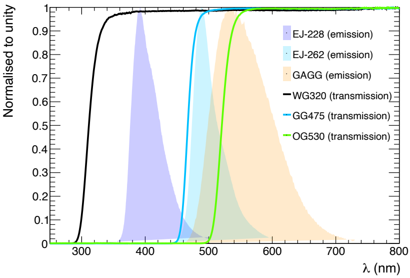

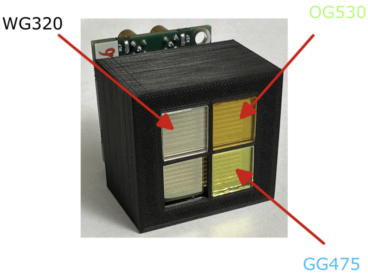

- What is the signal collected?
  - Channel A (WG320): GAGG + EJ-262 + EJ-228
  - Channel B (GG475): GAGG + EJ-262
  - Channel C (OG530): GAGG

Proof of concept – Signal

- Signal emitted by the different scintillating layers

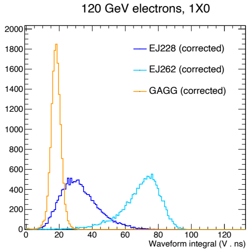

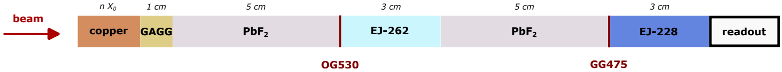

- With 120 GeV electrons, shower develops mostly in EJ-262 and EJ-228

Proof of concept – Signal

- Signal emitted by the different scintillating layers

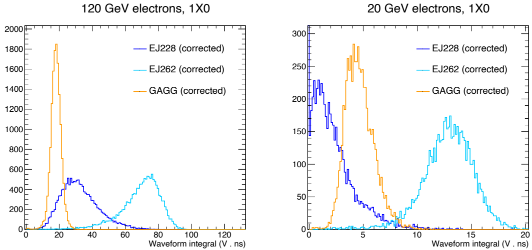

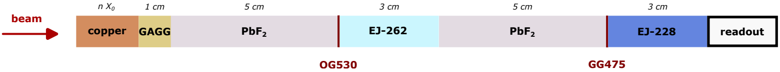

- With 120 GeV electrons, shower develops mostly in EJ-262 and EJ-228
- With 20 GeV electrons, shower develops mostly in EJ-262 and GAGG

Proof of concept – Signal

- Signal emitted by the different scintillating layers

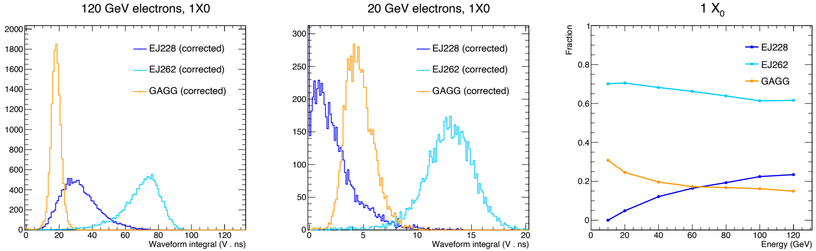

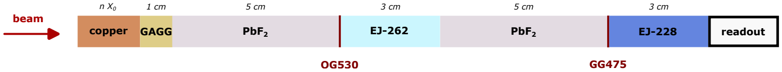

- The fraction of the signal of scintillator j is defined as

$$f_j = \frac{\mu_j}{\sum_i \mu_i}, \qquad i \in [\text{EJ-228}, \ \text{EJ-262}, \ \text{GAGG}]$$

where μ_i is the mean of the pulse integral distribution

- The greater the energy,
  - the greater the EJ-228 signal
  - the smaller the GAGG signal

Proof of concept – Shower profile

- Shower profile obtained by computing the centre-of-gravity, g, of the shower:

$$g = \sum_i f_i X_i, \qquad i \in [\text{EJ-228}, \ \text{EJ-262}, \ \text{GAGG}]$$

where f_i is the fraction of scintillator i and X_i the length up to scintillator i, in units of X_0

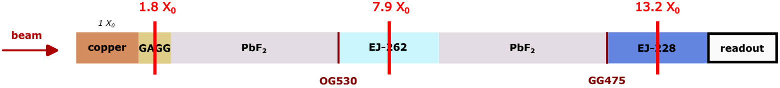

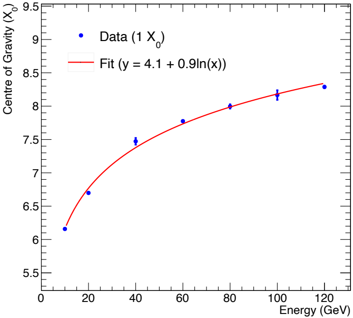

- The trend in energy is logarithmic, as expected
- This demonstrates the capability of the CCAL to resolve the longitudinal shower profile!
  - Not possible with non-segmented homogeneous calorimeters

Towards CCAL using nanocomposites

- Can the performance of the CCAL be enhanced using nanocomposites?

nanocomposite = quantum dots (semiconductor nanocrystals)
embedded in a transparent host material (matrix)

- The use of nanocomposites is well-motivated as the nanocrystals exhibit
  - Narrow emission spectrum
  - Tunable emission wavelength
  - Fast timing capabilities

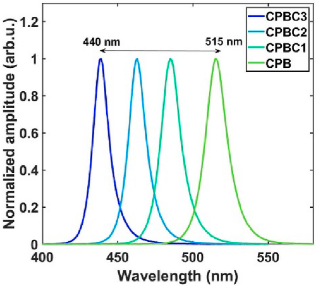

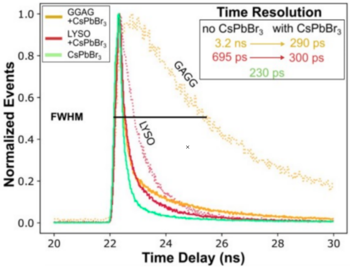

Figures from [*doi*]

Materials

- During the test beam, nanocomposites developed by the Czech Technical University in Prague were tested [doi]
- Two types of cesium lead halide nanocrystals were produced
  1. Cesium lead bromide (CPB)
  2. Cesium lead bromochloride (CPBC)

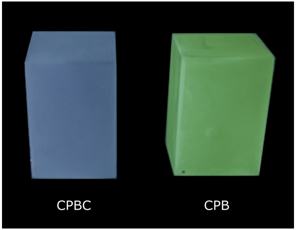

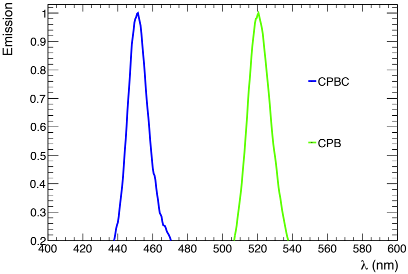

- Nanocrystals embedded in polysterene (PS) matrix

Optical properties

- Comparison of the waveform integral between
  - CPBC sample
  - CPBC sample with a long-pass filter with a cut-off at 495 nm (GG495)
  - Blank PS sample with a long-pass filter with a cut-off at 495 nm (GG495)
- CPBC scintillates at ~ 450 nm $\Rightarrow$ no light expected to be collected with the filter
- The fact that we nevertheless collect a signal suggests
  - Negligible direct excitation of the quantum dots within the matrix
  - Signal comes from Cherenkov emission of the PS matrix

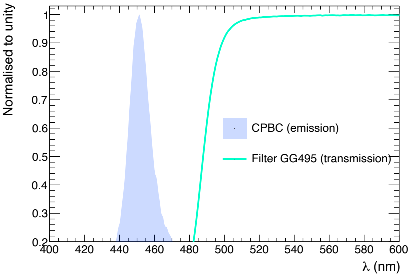

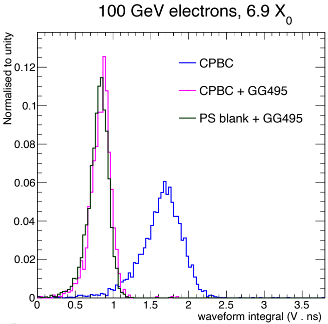

Nanocomposites as wavelength shifters

- With the current state of the art, nanocomposites cannot be used as scintillators, as the light output is limited by
  - Energy deposition in the nanocrystal tends to be too small direct excitation
  - Inefficient energy transfer from matrix
  - Self-absorption of light emitted by nanocrystals

Instead, can nanocomposites be used as wavelength shifters (WLS)?

- Samples were tested during the test beam at SPS in April 2026
  - 2 mm think cesium lead halide nanocrystals embedded in PDMS matrix
- CCAL prototype using WLS layers was tested with electron, pion, and muon beams
  - Data are being analysed

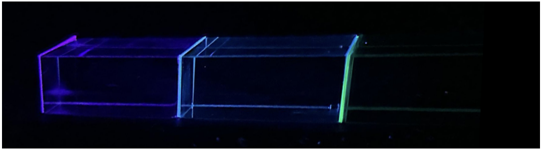

⇒ **Stay tuned !**

Outlook

- The chromatic calorimetry is a promising concept for the future of particle sensing
- Future steps include
  - Validate the concept of CCAL using WLS
  - Study the energy and time resolution
  - Design a calorimeter with more than one
  - And many more...

- Nanocomposites can be used beyond calorimetry
  - Idea for a chromatic tracking improving the resolution of the vertex reconstruction (2510.25667)

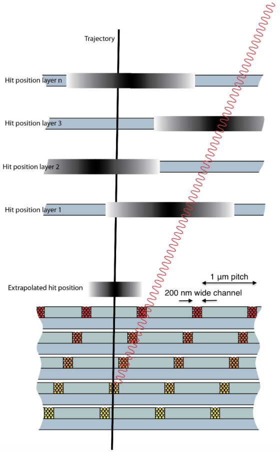

Summary

1. The collection of the B-parking data set opened a new avenue to study beauty decays at CMS

- First search for long-lived heavy neutrinos was performed
  - Achieves leading sensitivity for low-GeV signal

2. It was demonstrated that precision measurements in all-hadronic final states was possible at CMS

- Time-dependent measurement of CP violation in $B_s \rightarrow \phi(K^+K^-)\phi(K^+K^-)$ decays is ongoing

3. Using nanocomposites to enhance the performance of detectors is promising

- First prototypes for a chromatic calorimeter are being tested

$\Rightarrow$ **A lot of exciting results to come !**

Thank you !

Backup

Interpretation

- Lower exclusion limits on $c\tau_\mathrm{N}$ are presented for 66 different mixing scenarios for $m_\mathrm{N} = 1$, 1.5, and 2 GeV.
- Mixing scenarios specified by the ratios $(r_e,\, r_\mu,\, r_\tau)$ defined as $r_\ell \equiv |V_{\ell\mathrm{N}}|^2/|V_\mathrm{N}|^2$, $\ell = (\mathrm{e},\, \mu,\, \tau)$
- The condition $r_e + r_\mu + r_\tau = 1$ allows the values to be shown in the form of ternary plots

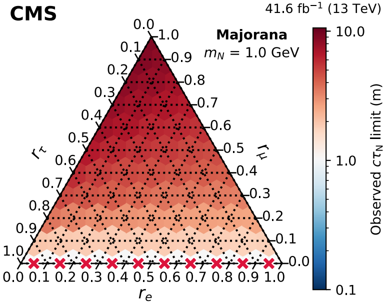

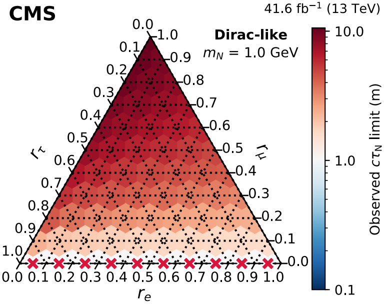

$\Rightarrow$ **First time that this type of constraints is presented for $m_\mathrm{N} \leq 2$ GeV**

Acceptance

- Additionally, a filter on the kinematic acceptance of the final state is applied
  - $p_{\mathrm{T}}(\mathrm{K}_i) > 0.5$ GeV and $|\eta|(\mathrm{K}_i) < 2.5$ ($i = 1, ..., 4$)
- Acceptance equals to 39.0%

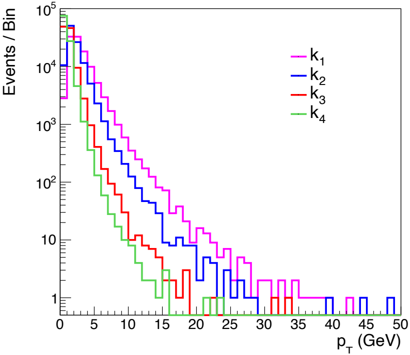

- Soft p_{T} signatures represents a challenge for the measurement

Experimental setup

- The CCAL prototype was tested in September 2025 at the SPS
- Several high-energy beams were used
  - Electrons at 10, 20, 40, 60, 80, 100, and 120 GeV
  - Charged pions at 80 GeV

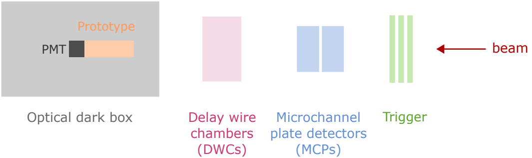

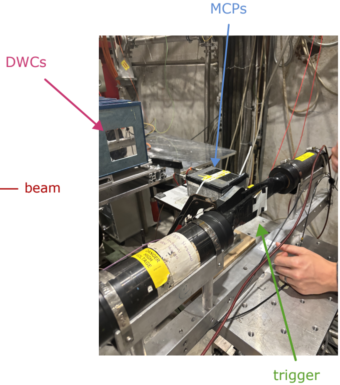

- Alignment of the various devices was checked before data taking

Experimental setup

- The CCAL prototype was tested in September 2025 at the SPS
- Several high-energy beams were used
  - Electrons at 10, 20, 40, 60, 80, 100, and 120 GeV
  - Charged pions at 80 GeV

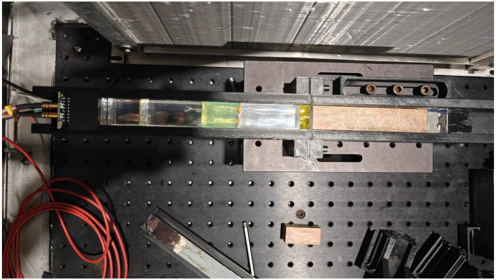

Picture of optical dark box

- 3D-printed holder that fits the dimensions of the CCAL prototype
- Inner part of the holder coated with Enhanced Specular Reflector (ESR) to minimise light losses

PMT signal

- Events are selected based on (i) the time and amplitude of the MCPs, (ii) the time of the PMT, and (iii) the spatial position of the shower
- Integral of the waveform taken as a figure of merit

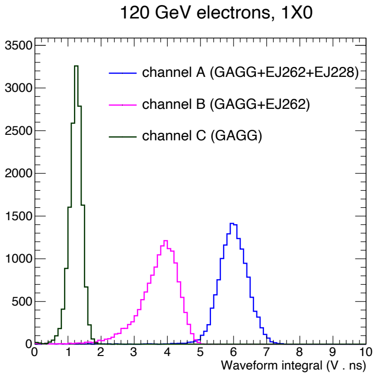

- As expected, filters with shorter cut-off wavelengths transmit more light, resulting in a larger integral value.
- How to convert the per-channel signal into the per-scintillator signal?

Scintillator signal – Strategy

- Naive approach to retrieve the per-scintillator signal:

Per-channel	Per-scintillator
▶ Channel A: GAGG + EJ-262 + EJ-228	▶ GAGG = channel C
▶ Channel B: GAGG + EJ-262	▶ EJ-262 = channel B - channel C
▶ Channel C: GAGG	▶ EJ-228 = channel A - channel B

- However, a series of corrections must be applied to account for the material and CCAL prototype properties

Scintillator signal – Strategy

- Naive approach to retrieve the per-scintillator signal:

Per-channel	Per-scintillator
▶ Channel A: GAGG + EJ-262 + EJ-228	▶ GAGG = channel C
▶ Channel B: GAGG + EJ-262	▶ EJ-262 = channel B - channel C
▶ Channel C: GAGG	▶ EJ-228 = channel A - channel B

- However, a series of corrections must be applied to account for the material and CCAL prototype properties

1. Transport coefficient
   - 100% of the light emitted by the EJ-228 reaches the PMT
   - 72.3% of the light emitted by the EJ-262 reaches the PMT
   - 34.2% of the light emitted by the GAGG reaches the PMT

Scintillator signal – Strategy

- Naive approach to retrieve the per-scintillator signal:

Per-channel	Per-scintillator
▶ Channel A: GAGG + EJ-262 + EJ-228	▶ GAGG = channel C
▶ Channel B: GAGG + EJ-262	▶ EJ-262 = channel B - channel C
▶ Channel C: GAGG	▶ EJ-228 = channel A - channel B

- However, a series of corrections must be applied to account for the material and CCAL prototype properties

1. Transport coefficient
2. PMT acceptance
   - ▶ Convolution of the PMT quantum efficiency (QE) with the scintillator's emission

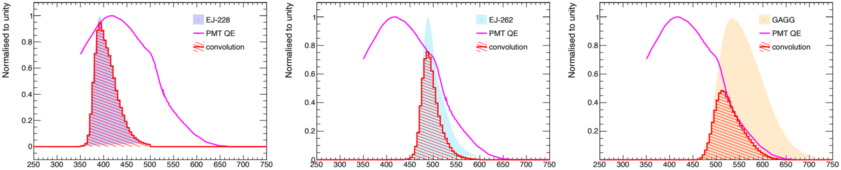

Scintillator signal – Strategy

- Naive approach to retrieve the per-scintillator signal:

Per-channel	**Per-scintillator**
▶ Channel A: GAGG + EJ-262 + EJ-228	▶ GAGG = channel C
▶ Channel B: GAGG + EJ-262	▶ EJ-262 = channel B - channel C
▶ Channel C: GAGG	▶ EJ-228 = channel A - channel B

- However, a series of corrections must be applied to account for the material and CCAL prototype properties

1. Transport coefficient
2. PMT acceptance
3. Reflection properties
   - ESR placed at the back of GAGG
     ⇒ $\sim$ 100% of the GAGG light goes to the PMT
   - No ESR placed at the back of EJ228 and EJ262
     ⇒ $\sim$ 50% of the EJ light goes to the PMT

Scintillator signal – Strategy

- Naive approach to retrieve the per-scintillator signal:

Per-channel	Per-scintillator
Channel A: GAGG + EJ-262 + EJ-228	GAGG = channel C
Channel B: GAGG + EJ-262	EJ-262 = channel B - channel C
Channel C: GAGG	EJ-228 = channel A - channel B

- However, a series of corrections must be applied to account for the material and CCAL prototype properties

1. Transport coefficient
2. PMT acceptance
3. Reflection properties
4. Scintillator light yield
   - Defined as the number of photons produced per unit of energy deposited
   - Relative light yield of the scintillators
     - EJ-228 : EJ-262 : GAGG = 1 : 1.06 : 2.46

Experimental setup

- The various nanocomposites were tested with electron beams with energy between 20 and 100 GeV and several lengths of the copper absorber

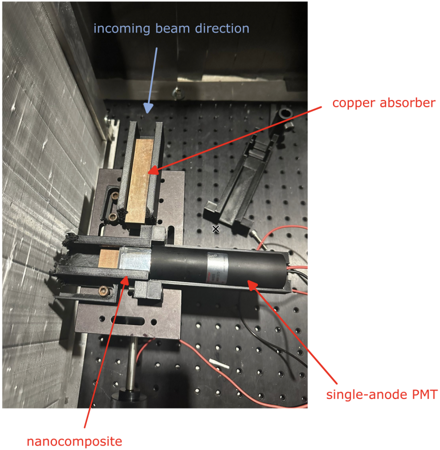

Energy

- Linear response of the signal with the energy

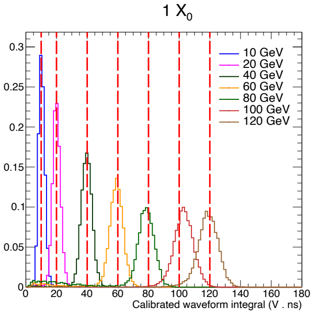

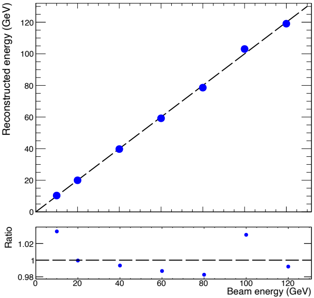

Proof of concept – Particle identification

- Can the CCAL discriminate between different incoming particles?
  - Compare performance obtained with pion and electron beams at 80 GeV
- Study correlation between the fraction in GAGG and EJ-262

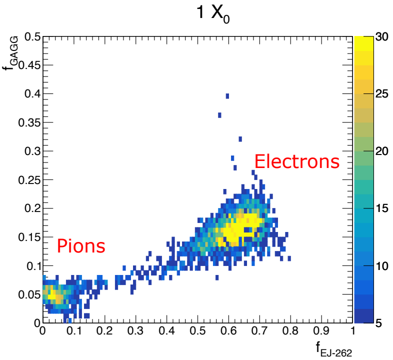

- Particles can be discriminated based on the fraction correlation
  - Electrons leave more energy in EJ-262 compared to the pions

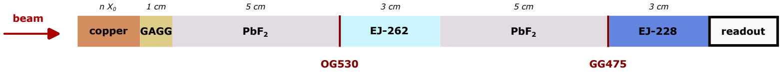

Host material

- To produce the nanocomposites, the nanocrystals are embedded in two types of organic polymers
  1. Polysterene (PS)
  2. Polyurethane
- Novel surface treatment developed to obtain transparent samples at higher loading levels

Polyurethane samples